Journal of Medicinal Chemistry

Article

pubs.acs.org/jmc

Ruthenium−Arene Complexes of Curcumin: X-Ray and Density Functional Theory Structure, Synthesis, and Spectroscopic Characterization, in Vitro Antitumor Activity, and DNA Docking Studies of (*p*-Cymene)Ru(curcuminato)chloro

Francesco Caruso,*[,†] Miriam Rossi,*[,‡] Aidan Benson,[‡] Cristian Opazo,[§] Daniel Freedman,[∥] Elena Monti,[⊥] Marzia Bruna Gariboldi,[⊥] Jodi Shaulky,[#] Fabio Marchetti,[▽] Riccardo Pettinari,[○] and Claudio Pettinari[○]

[†]Istituto di Chimica Biomolecolare, Consiglio Nazionale delle Ricerche, c/o University of Rome "La Sapienza", Istituto Chimico, Piazzale Aldo Moro 5, 00185, Rome, Italy

[‡]Vassar College, Department of Chemistry, Poughkeepsie, New York 12604, United States

[§]Vassar College, Academic Computing Service, Poughkeepsie, New York 12604, United States

[∥]State University of New York, Department of Chemistry, New Paltz, New York 12561, United States

[⊥]University of Insubria, Department of Structural and Functional Biology, Via A. da Giussano 10, 21052 Busto Arsizio, Varese, Italy

[#]Accelrys, Inc., 10188 Telesis Court, Suite 100, San Diego, California 92121, United States

[▽]School of Science and Technology, Università degli Studi di Camerino, via S. Agostino 1, 62032 Camerino MC, Italy

[○]School of Pharmacy, Università degli Studi di Camerino, via S. Agostino 1, 62032 Camerino MC, Italy

Supporting Information

ABSTRACT: The in vitro antiproliferative activity of the title compound on five tumor cell lines shows preference for the colon−rectal tumor HCT116, IC_{50} = 13.98 μM, followed by breast MCF7 (19.58 μM) and ovarian A2780 (23.38 μM) cell lines; human glioblastoma U-87 and lung carcinoma A549 are less sensitive. A commercial curcumin reagent, also containing demethoxy and bis-demethoxy curcumin, was used to synthesize the title compound, and so (*p*-cymene)Ru(demethoxy-curcuminato)chloro was also isolated and chemically characterized. The crystal structure of the title compound shows (1) the chlorine atom linking two neighboring complexes through H-bonds with two O-(hydroxyl), forming an infinite two-step network; (2) significant twist in the curcuminato, 20° between the planes of the two phenyl rings. This was also seen in the docking of the Ru-complex onto a rich guanine B-DNA decamer, where a Ru−N7(guanine) interaction is detected. This Ru−N7(guanine) interaction is also seen with ESI-MS on a Ru-complex-guanosine derivative.

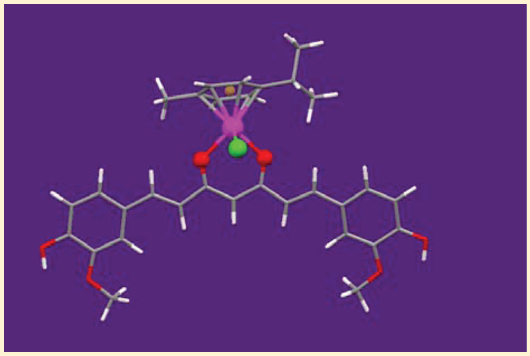

INTRODUCTION

Cancer is the second leading cause of death in economically developed countries and the third in emergent nations.[1] Although survival rates have increased due to efficient anticancer drugs and prevention, many types of cancer still have no effective cure. Most new therapeutic candidates are organic compounds, yet metal complexes are of interest because metal ions are essential in many natural biological processes. Notably, metal complexes offer mechanisms of action that are unavailable to organic compounds. The nature of the metal ion, its oxidation state (including multiple redox modifications), and the type and number of bound ligands can exert a critical influence on the biological activity of a metal complex.[2] A turning point for the use of metal antitumor agents was the development of the platinum-based drugs that provide well established treatments, although limited by toxicity and drug resistance.[3] The search for other metal drug anticancer agents drives much current research interests,[4] with particular attention to ruthenium.[5]

Two Ru[III] species, NAMI-A(antimetastatic)[6]and KP1019,[7] are in clinical trials. Ru(II) arene complexes appear to have an altered profile of biological activity in comparison with metal-based anticancer complexes currently in clinical use.[8] The ligand exchange kinetics of Pt(II) and Ru(II) complexes in aqueous solution, crucial for anticancer activity, are very similar.[9] Moreover, ruthenium compounds are not very toxic and some are quite selective for cancer cells, likely due to the ability of ruthenium to mimic iron in binding to biomolecules.[10] Sadler and Dyson have explored the activity of neutral or

Received: July 11, 2011
Published: December 29, 2011

cationic "half-sandwich" arene Ru(II) complexes;[11,12] these often possess good aqueous solubility (useful for clinical use) and the arene ligand is relatively inert toward displacement under physiological conditions.[13,14] Cationic arene ruthenium ethylenediamine complexes reported by Sadler show very high activity both in vitro and in vivo.[15−17] Their interaction with DNA model compounds and other biologically relevant molecules has been established through simultaneous covalent coordination, intercalation of extended aromatic groups and stereospecific hydrogen bonding.[18−21] Arene ruthenium complexes containing phosphine ligands, such as pta (1,3,5-triaza-7-phosphatricyclo[3.3.1.1]decane), as well as *N*,*O*- or *O*,*O*-chelating ligands, such as carboxylates, resist hydrolysis, yet this phenomenon does not diminish cytotoxicity.[22−25] However, limited efforts have been made in conjugating the metal center with ligands that themselves show biological activity. It was for this reason that we are investigating the chemistry and potential antitumor activity of novel Ru(II)−(arene) compounds with a variant of β-diketonato ligands, curcumin, a well-known natural compound whose coordination chemistry has been only partially explored.[26−29] Systematic investigations of curcumin reveals a wide spectrum of beneficial properties including antioxidant, anti-inflammatory, antimicrobial, and anticancer activities.[30,31] In addition, it protects neurons against β-amyloid peptide toxicity and binds to β-amyloid plaques of transgenic mouse models of Alzheimer's disease.[32,33] In continuation of our previous exploration of Ru(II)−(arene) chemistry with β-diketones,[34] and considering the interesting biological properties of curcumin, we report the chemical characterization of several Ru−(arene)−curcuminato complexes and the molecular structure of [(*p*-cymene)Ru(curcuminato)chloro] along with its antitumor activity on five tumor cell lines in vitro. We also describe docking experiments of this complex onto a guanosine rich DNA substrate.

RESULTS AND DISCUSSION

Synthesis and Characterization of Complexes. Derivative **1**, Ru-Cur, is obtained by interaction of commercial curcumin and $[(p\text{-cymene})RuCl_2]_2$ in methanol in the presence of NaOMe; consequent TLC separation using a mixture of chloroform/methanol (9:1) as eluent gave its composition as [(*p*-cymene)Ru(curcuminato)Cl] (Scheme 1).

Scheme 1

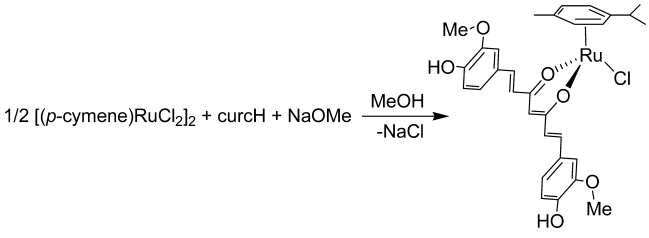

The compound is an air and moisture stable orange solid, soluble in chlorohydrocarbon, alcohol, acetone, acetonitrile, and DMSO solvents, where they are partially dissociated, as indicated by eq 1:

$$[(p\text{-cymene})Ru(curcuminato)chloro] + S(solvent) \leftrightarrows [(p\text{-cymene})Ru(curcuminato)(S)]^+ + Cl^- \quad (1)$$

Ru-Cur is rather insoluble in water. Upon prolonged standing in deuterated-water suspension, a small portion (5%) decomposed toward neutral curcumin and Ru(*p*-cymene)(Solv)$_x$Cl species, the remaining 95% being unaltered. Thus, the ^{1}H NMR (D_2O) spectrum of Ru-Cur shows only signals due to *p*-cymene moiety, in accordance with the observations reported in the literature.[35]

The IR spectrum of **1** shows the typical ν(O−H) and ν(C═O, C═C) bands of curcumin shifted to lower wavenumbers as a consequence of its metal coordination through both carbonyl arms. The ^{1}H and $^{13}C\{^1H\}$ NMR spectra of **1** contain all the expected resonances of the (*p*-cymene)Ru(II) fragment and of the curcuminato ligand (the numbering of C atoms in curcumin is indicated in Scheme 2), in a 1:1 ratio in accordance with the

Scheme 2

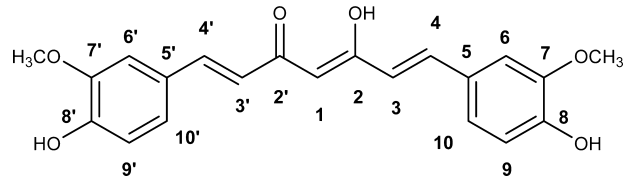

stoichiometry of proposed derivatives. The positive ESI-MS spectra of Ru-Cur, carried out in methanol or acetonitrile, display the peak corresponding to [(*p*-cymene)Ru(curcuminato)]$^+$, while those carried out on the crude product prior the TLC separation contain also the peaks due to derivatives containing demethoxycurcumin and bis(demethoxy)curcumin.

Using the same previously described TLC separation procedure, we were able to isolate derivative **2** (*p*-cymene)Ru(demethoxycurcuminato)chloro which originated from the small fraction of the demethoxycurcumin (d-curcH) in the commercial ligand. It displays similar spectral features with some differences in the proton spectrum due to the absence of a methoxy group in the O_2-chelating ligand.

To ascertain the ability of Ru-Cur to interact with nucleic acid bases, we have performed an ESI-MS study on a methanol solution containing a 1:1 mixture of Ru-Cur and 9-ethylguanine. The positive ESI spectrum shows a *m*/*z* peak at 782 corresponding to [(*p*-cymene)Ru(curcuminato)(9-ethylguanine)]$^+$, and an additional peak at 450 due to [(*p*-cymene)RuCl(9-ethylguanine)]$^+$, thus confirming the ability of the ruthenium(II) fragment to coordinate the nucleobase. Similarly, the ESI-MS spectrum on a methanol solution, containing a 1:1 mixture of derivative **2** and 9-ethylguanine, showed a peak at 752 corresponding to [(*p*-cymene)Ru(demethoxycurcuminato)(9-ethylguanine)]$^+$, which further confirmed the coordination of the nucleobase to ruthenium.

Structural Data. The single crystal X-ray diffraction experiment yielded the molecular structure of the title compound and is depicted in Figure 1. Crystals gave weak diffraction and provided limited number of useful reflections; as a result, only some atoms could be refined anisotropically. The metal is bound to 2 O donors from the chelating β-diketone curcuminato, one Cl anion, and the *p*-cymene aromatic ring, thus forming a piano-stool arrangement, where both O-(curcuminato) and Cl are the legs. The curcumin ligand is twisted with a torsion angle about the coordination sphere O(6)−Ru(1)−O(5)−C(9) of 11.2°(1), while the angle between the planes of the two phenyl rings in curcumin is

dx.doi.org/10.1021/jm200912j | J. Med. Chem. 2012, 55, 1072−1081

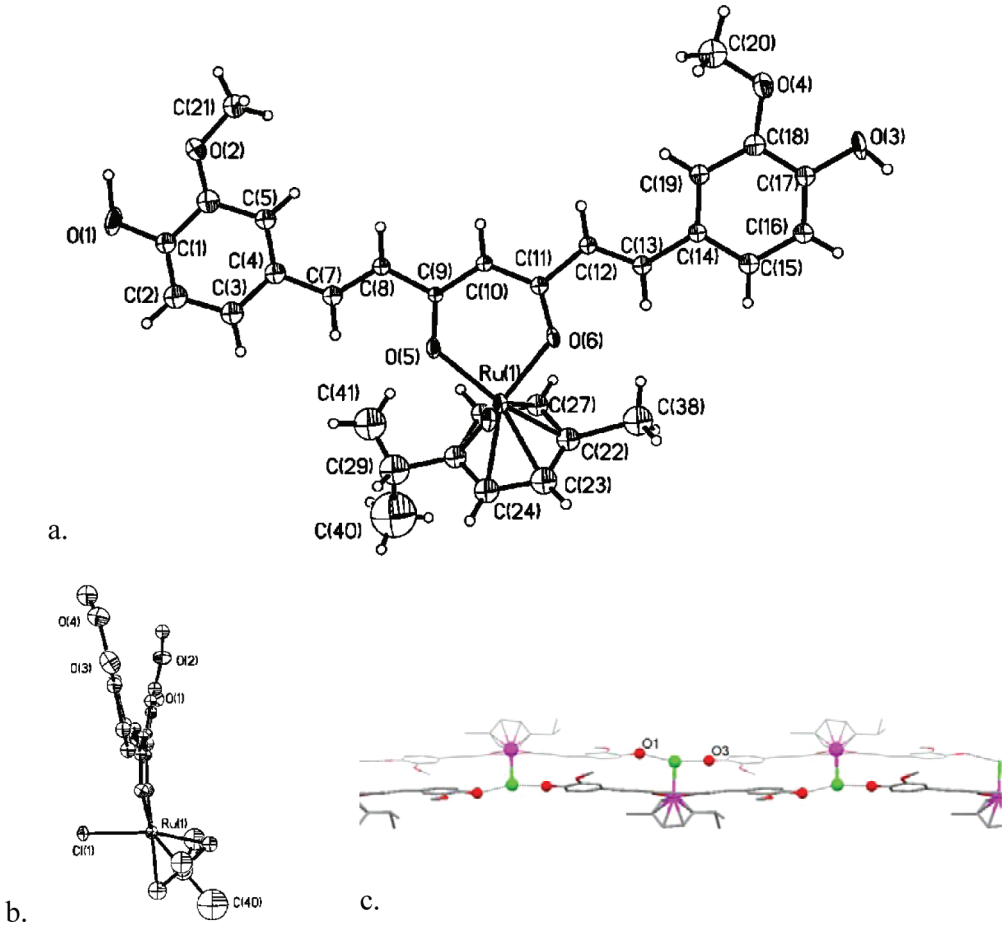

Figure 1. (a) X-ray molecular structure of the title compound, Ru-Cur. Disorder on the *i*-propyl goup of *p*-cymene is evident. (b) Profile view with H atoms omitted showing piano-stool geometry as well as the twist of the curcumin ligand; torsion angle about the coordination sphere O(6)−Ru(1)−O(5)−C(9) is 11.2°(1), while the angle between the planes of the two phenyl rings in curcumin is 20°. (c) In the packing of the molecule, the intermolecular interactions are such that each chlorine (green) atom forms two strong O···Cl-hydrogen bonds with neighboring complexes through their hydroxyl oxygen (red) atoms O(1) and O(3), thereby forming a parallel two-step ladder infinite network. One of the steps is shown in bold.

20° (see Figure 1b). Disorder of the *i*-propyl moiety in the *p*-cymene ring is seen by the large spherical isotropic displacement parameters on the lower left side of Figure 1a.

Using all non-H atom coordinates experimentally obtained from the X-ray study and the generated H atoms, we performed a DFT geometry-optimization on Ru-Cur. The converged structure, shown in Figure 2, is at a minimum of energy as all its calculated frequencies are positive. Specific comparison between the coordination sphere of the experimental and calculated structures indicates an excellent agreement of bond angles and slightly overestimated bond distances in the latter. Thus, the Ru−Cl bond length, 2.473 Å (DFT) is longer than 2.436(2) Å (X-ray), as are Ru−O data (DFT), around 2.10 Å and 2.07 Å, respectively; the Ru arene centroid is also slightly elongated: Ru−centroid of 1.747 Å and 1.65(2) Å, respectively. This DFT structure was later used for docking onto a DNA substrate.

Comparison between X-ray structures of the title compound and the related Ru complex of dimethoxy-curcumin, bis((1,7-bis(3,4-dimethoxyphenyl)-hept-1,6-diene-3,5-dione)-(η_6-*p*-cymene)-chloro-ruthenium(II),[36] in Table 1 indicates that replacement of both peripheral hydroxyls in the title compound by methoxy groups does not affect the coordination sphere, as expected; this confirms that our X-ray structure is reliable

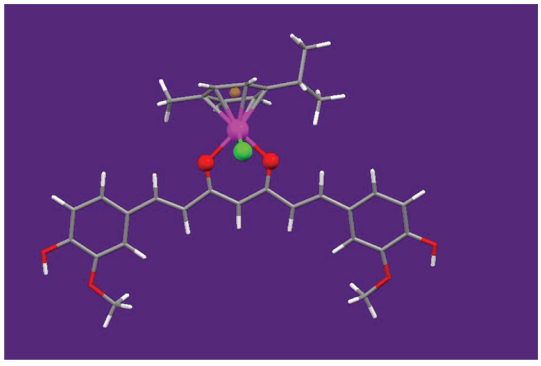

Figure 2. DFT molecular structure of Ru-Cur. Both H(hydroxyl) atoms were pointed toward their methoxy neighbors. Ru, both O(keto−enol) and Cl are ball and stick style, all other atoms are stick style. The *p*-cymene ring center is also indicated (yellow). The initial coordinates for all non-H atoms in this DFT minimized species were obtained from the X-ray study.

notwithstanding its high R_f crystallographic factor. There are 15 hits in the CSD database for (arene)Ru(chloro) β-diketonates and, compared to them, the title compound shows normal structural features. For instance, the Ru−arene centroid mean value is 1.648 Å, which compares well with our 1.65(2) Å,

dx.doi.org/10.1021/jm200912j | *J. Med. Chem.* 2012, 55, 1072−1081

Table 1. Structural Data in the Coordination Sphere of the 2 Molecules in the Asymmetric Unit of Bis((1,7-bis(3,4-dimethoxyphenyl)-hept-1,6-diene-3,5-dione)-(η_6-*p*-cymene)-chloro-ruthenium(II),[36] Named Ru-Dim-Cur, and the Title Compound (*p*-cymene)Ru(curcuminato)chloro, Named Ru-Cur, and the DFT Minimized Structure of the Latter

name/ technique	Ru-Dim-Cur X-ray (1)	Ru-Dim-Cur X-ray (2)	Ru-Cur X-ray	Ru-Cur DFT
Ru−Cl	2.435(1)	2.422(1)	2.436(4)	2.473
Ru−O	2.067(4)	2.066(4)	2.06(1)	2.098
	2.071(3)	2.073(3)	2.07(1)	2.100
Ru−centroid	1.646(4)	1.649(5)	1.65(2)	1.747
Ru−C(max)	2.198(5)	2.189(5)	2.20(2)	2.297
Ru−C(min)	2.142(4)	2.138(5)	2.07(2)	2.234
O−C	1.284(6)	1.274(7)	1.41(2)	1.294
	1.285(6)	1.277(6)	1.33(2)	1.294
C−C	1.381(7)	1.392(8)	1.38(2)	1.413
	1.397(7)	1.407(6)	1.40(2)	1.415
Cl−Ru−O	85.1(1)	84.3(1)	83.4(3)	84.7
	84.6(1)	84.7(1)	84.5(3)	85.6
O−Ru−O	88.3(1)	88.0(1)	87.3(4)	88.7
Cl−Ru−centroid	128.1(1)	128.1(1)	130.6(5)	128.5
O−Ru−centroid	128.1(1)	127.9(2)	126.2(6)	126.1
	127.8(1)	128.6(2)	129.2(6)	128.8

Table 1. The symmetric nature of the curcumin ligand is reflected in the coordination sphere, as both Ru−O-(curcuminato) bond lengths are equal [2.06(1), 2.07(1) Å], in contrast with the asymmetric *β*-diketonato ligand in (*p*-cymene)-chloro-(4-(trifluoroacetyl)-3-methyl-1-phenyl-pyrazol-5-onato)-ruthenium(II) that shows significantly different Ru−O bond lengths [2.095(1), 2.104(1) Å].[34]

As seen in Table 1, our structure shows a Ru−Cl bond length (2.436(4)Å) similar to that in the dimethoxycurcumin derivative. The packing of our molecule shows the chlorine atom having a key role in the intermolecular interactions because it links two neighboring complexes through two strong O−H···Cl-hydrogen bonds with their hydroxyl oxygen atoms O(1)···Cl 3.100(5) Å and O(3)···Cl 3.128(5) Å and thereby forming an infinite two-step network, as seen in Figure 1c. The step distance is the Ru−Cl bond distance while the separation between the two-step network is graphite-like, with the shortest (C(4)···C(15′)) stacking interaction distance of 3.374(5) Å. This stacking occurs down the crystallographic *b* axis between two curcumin-phenyl rings. The solvent water molecule, which is on a 2-fold axis of symmetry, lies at the apex of a distorted square pyramid with two hydrogen bonded (2.902(5) Å) methoxy O(2) atoms at opposite corners of the square base and two weaker interactions with the two hydroxyl oxygen O(1) atoms at the remaining two corners at 3.358(5) Å.

Biological Activity. The title compound was initially tested on five tumor cell lines. Figure 3 shows these results for the most sensitive three lines while the dose-dependent behavior is shown in Supporting Information Figure S8, specific IC_{50} values are presented in Table 2. The activity of the title compound on the ovarian tumor cell line A2780 yields an IC_{50} value similar to that reported for the cationic complex [(hexamethylbenzene)Ru(ethylendiamine)(NCS)]$^+$ (23.38 ± 3.334 μM vs 24 μM, respectively).[37] A more specific comparison with related *β*-diketonato Ru complexes, that contain the same *p*-cymene arene, shows an IC_{50} of 19 μM for [(*p*-cymene)Ru(R1C(O)CHC(O)R2)Cl] (R1 = CH_3, R2 = H), 14 μM (R1 = *t*-Bu_3, R2 = H), 11 μM (R1 = Ph, R2 = H),[23] 24 μM (R1 = CH_3, R2 = Cl).[38] Also the lung carcinoma A549 cell line shows values similar to those reported in the literature for [(*p*-cymene)Ru(R1C(O)CHC(O)R2))(Cl)], R1 = CH_3, R2 = Cl.[38] The highest activity for Ru-Cur was observed in the human colorectal carcinoma cell line HCT116 (CCL-247), 13.98 ± 1.503 μM, which can be compared to 8 μM obtained for the ethylenediamine−Ru chelate cationic species [($C_6H_5C_6H_5$)RuCl ($H_2NCH_2CH_2NH_2$-*N*,*N*′)]$^+$ PF_6^- in the same cell line.[39] Interestingly, ethylenediamine Ru chelates are considered better antitumor agents than Ru-*β*-diketonates.[13] SW480 is another colon−rectal cell line in which Ru compounds of the type [(*p*-cymene)Ru(oxine)(Hazole), oxine = deprotonated 8-hydroxyquinoleine, Hazole = azole heterocycle, were investigated. For these highly active antitumor compounds, the range of activity is 3.3−15.3 μM,

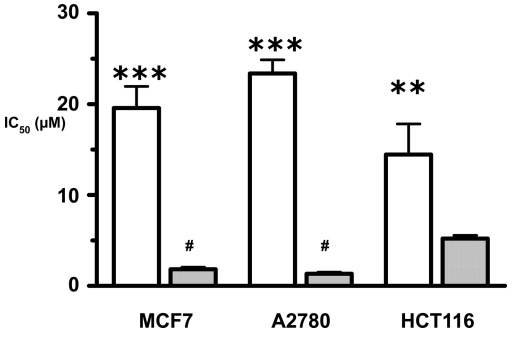

Figure 3. Effect of 72 h exposure of MCF7 (breast), A2780 (ovarian), and HCT116 (colon) cancer cells to Ru-Cur (empty bars) and cisplatin (CDDP, hatched bars). Means ± SE of 4−6 independent experiments. *** $p < 0.001$ vs CDDP; ** $p < 0.01$ vs CDDP; # $p < 0.001$ vs HCT116.

Table 2. IC_{50} (μM) Values of the Title Compound Ru-Cur and Cisplatin in Several Tumor Cell Lines (*n* = Number of Experiments Performed)

	cancer line	Ru-Cur mean ± SD (*n*)	cisplatin mean ± SD (*n*)
MCF7	breast adenocarcinoma	19.58 ± 2.367 (5)	1.835 ± 0.237 (5)
HCT116	colon adenocarcinoma	13.98 ± 1.503 (6)	5.217 ± 0.348 (5)
A2780	ovarian carcinoma	23.38 ± 3.334 (4)	1.325 ± 0.196 (5)
CP8	ovarian platinum-resistant	27.00 ± 2.332 (5)	9.918 ± 1.155 (5)
A549	lung adenocarcinoma	62.33 ± 8.934 (4)	
U87	glioblastoma	29.36 ± 1.842 (3)	

dx.doi.org/10.1021/jm200912j | J. Med. Chem. 2012, 55, 1072−1081

with the most active species having Hazole = imidazole; similar activity was found for the ovarian carcinoma CH.[40] Moreover, related compounds have submicromolar range of activity for the A549 lung carcinoma cell line.[41] In contrast, the title compound shows the least activity toward A549, 62.33 ± 8.934 μM, whereas glioblastoma U87 has intermediate activity, 29.36 ± 1.842 μM.

The effects of Ru-Cur on the three most sensitive cell lines tested, MCF7, A2780, and HCT116, were compared with those elicited by cisplatin, the prototypical metal-based anticancer drug, also shown in Table 2. It should be noted that HCT116 cells are deficient in mismatch repair function, due to a hemizygous mutation in the hMLH1 gene, resulting in a truncated, nonfunctional protein;[42] this defect plays a major role in determining the relative resistance of this cell line to cisplatin.[43] The results of this comparative evaluation indicate that while cisplatin is significantly more potent than Ru-Cur on all three cell lines, its effects on the colon carcinoma cell line are somewhat inferior to those observed for the other cell lines tested, as expected; in contrast, the effects of Ru-Cur do not seem to depend on mismatch repair proficiency of the tumor cells, as indicated by the absence of significant differences in the IC_{50} values obtained for the three cell lines (Figure 3). To compare the therapeutic windows of Ru-Cur and cisplatin, we tested the two compounds on the nonmalignant human breast cell line MCF-10A and compared the results with those obtained for MCF7 cells. The following IC_{50} values were obtained: 19.06 ± 2.37 μM in MCF7 vs 102.1 ± 6.5 μM in MCF-10A for Ru-Cur; 1.83 ± 0.24 μM in MCF7 vs 7.27 ± 0.56 μM in MCF-10A for cisplatin. Thus, both compounds are approximately 4- to 5-fold more potent on carcinoma cells as compared to nonmalignant cells derived from the same tissue.

Interestingly, when Ru-Cur and cisplatin were tested on a variant cell line selected from A2780 for its resistance to cisplatin (CP8),[44] the effects of Ru-Cur were similar to those observed in the parental cell line, thus confirming the absence of cross-resistance between the two compounds (Figure 4, Table 2). This observation fits nicely with what has been reported above about the effects of cisplatin and Ru-Cur on HCT116 cells. Mismatch repair defects are among the major mechanisms involved in acquired resistance to cisplatin in A2780 cells;[45] thus, the observation that Ru-Cur is about as potent on cisplatin-sensitive as on cisplatin-resistant A2780 cells supports the notion that its activity is independent of mismatch repair status.

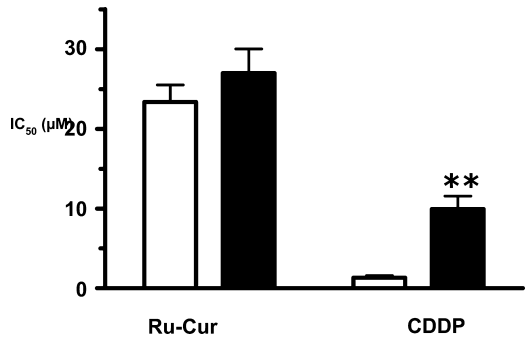

Figure 4. Effect of 72 h exposure to Ru-Cur and cisplatin (CDDP) in platinum-sensitive (A2780, empty bars) and -resistant (CP8, filled bars) human ovarian cancer cells. Means ± SE of 4–5 independent experiments. ** $p < 0.01$ vs A2780.

Comparison of Ru-Cur activity with curcumin (Figure 5) shows that, while curcumin is significantly more potent on MCF7 and A2780 cells, the IC_{50} values obtained for the two compounds in HCT116 cells and in the cisplatin-resistant ovarian line do not significantly differ from one another. Interestingly, this latter cell line is significantly less responsive to curcumin as well as to cisplatin, the resistance index (RI = IC_{50}[A2780]/IC_{50}[CP8]) for curcumin being approximately 3; in contrast, as already mentioned above, Ru-Cur is roughly as potent on resistant as on sensitive cells (R.I. ≈1).

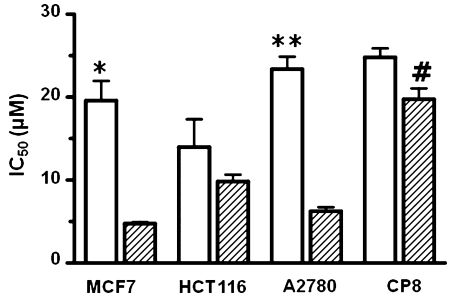

Figure 5. Effect of 72 h exposure of MCF7 (breast), HCT116 (colon), and A2780 and CP8 (both from ovary) cancer cells to RuCUR (empty bars), and curcumin (hatched bars). Means ± SE of 3–6 independent experiments. * $p < 0.05$ vs curcumin ** $p < 0.01$ vs curcumin. # $p < 0.01$ vs all other cell lines exposed to curcumin.

Docking on DNA. Bonding between Ru and N7(guanine) is considered the predominant mode of action with DNA for Ru antitumor compounds.[46] Indeed, this interaction is shown to be specific as only some guanine N7 sites are preferred. Thus, in the self-complementary d(CGGCCG) nucleotide, only G3 and G6 are ruthenated by a (*p*-cymene)Ru(ethylenediamine) species, while in the equivalent single strand nucleotide all guanines were reactive.[47] Therefore we decided to study a rich-guanine polynucleotide as a receptor to explore a docking of the title compound. Using Discovery Studio 3.0, we built an ab initio double helix B DNA decamer containing only alternant C-G bases, whose helices were named as "A" and "S". Counterions were imposed to hold a neutral system receptor. The docking process suggests that indeed Ru–N7(guanine) interaction is feasible, as depicted in Figure 6, see also Experimental Section.

In addition, interaction between Ru and O(phosphate) for the same Guanosine6 "(A)" nucleotide was also apparent, shown in Figure 7, and this (*p*-cymene)Ru(curcuminato)-decamer has a molecular energy very similar to that of the corresponding Ru–N7(guanine) species shown in Figure 6. However, the literature has a large amount of data supporting Ru–N7(guanine) binding. For instance, the non-natural species 9-ethylguanine was used to mimic the DNA N7-(guanine)-Ru bonding, as shown crystallographically in the cationic compound [(biphenyl)Ru(ethylethylenediamine-*N,N'*)(9-ethylguanine)].[46] This interaction was also confirmed using the natural nucleoside guanosine in the crystalline cationic species [(biphenyl)Ru(ethylenediamine)-(guanosine)], whereas the use of guanosinemonophosphate, GMP, allowed verification of the Ru–N7(guanine) bonding using NMR.[46] Moreover, in a more recent study of Ru-β-diketonates, the cationic compound [(*p*-cymene)Ru(Ph_2acac)(9-ethyl-guanine-N7)]$^+$ also shows Ru–N7(guanine) bonding.[48]

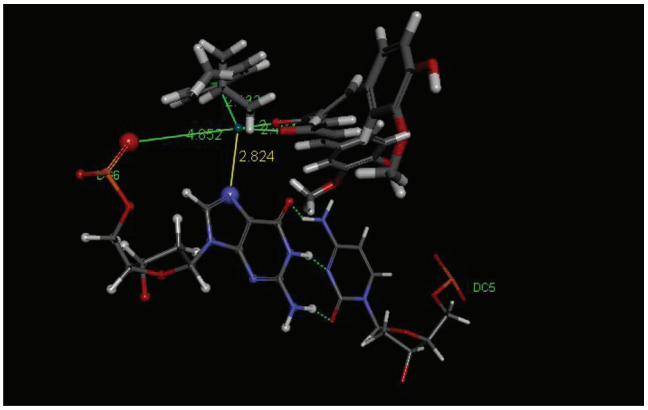

Figure 6. Minimization of conformer no. 155, from a standard dynamic cascade where all nucleotides were not fixed (except those terminal), showing a good approach of N7(guanine-"A") to the metal (2.824 Å). Only one pair of complementary nucleotides of the receptor decamer C−G are shown, Guanosine6 ("A") and its paired Cytosine5 ("S"), labeled DG6 and DC5. The setting of this minimization was the same for the standard dynamic cascade protocol, shown in the Experimental Section; such process holds the complete H-bond pairing, as shown. The Ru---O(phosphate) separation of 4.852 Å is also shown for later discussion.

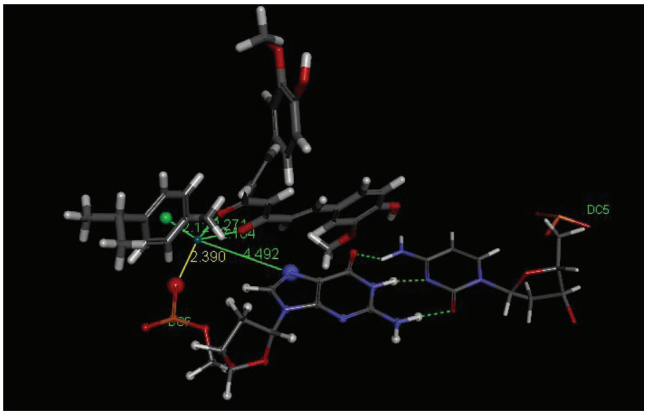

Figure 7. Minimization of conformer no. 351, from a standard dynamic cascade where only terminal nucleotides were fixed, showing a potential interaction between Ru and O(phosphate) (2.390 Å). This minimization process holds the H-bond pairing as depicted.

We suggest that, as no experimental evidence exists, the Ru−O(phosphate) interaction, although not absolutely excluded, could be a consequence of the lack of appropriate Ru functions in the molecular mechanics algorithm employed during the docking technique. This is also suggested by the experimentally Ru−N7 guanine derivative detected in this work using ESI-MS, see above.

CONCLUSIONS

Cisplatin and other Pt antitumor drugs are well established in the treatment of testes, ovarian, and lung cancer, but thus far, other tumors resist treatment by metal complexes. Gastrointestinal tumors are increasingly of concern in humans, and the title compound shows excellent activity on the colon−rectal tumor cell line HCT116, IC_{50} = 13.98 ± 1.503 μM. This Ru[II] complex contains the natural product curcumin as a β-diketonato ligand, which has been used extensively as a food component in Asian cultures and as ethnic medicine; its recognized benefits for health makes this natural product an attractive ligand for metal coordination, so far almost unexplored. Our Ru−curcuminato complex also shows good antitumor activity in breast MCF7 (19.58 ± 2.367 μM) and ovarian A2780 (23.38 ± 3.334 μM) cell lines, while human glioblastoma U-87 and lung carcinoma A549 are less sensitive. This indication of selectivity is considered a positive feature for further development. A docking study of the title compound on a guanine-rich DNA decamer shows metal interaction with N7−guanine and O(phosphate); the former supported experimentally by many studies, including this work. The Ru−N7 binding is supported also by the fact that Ru−Cl bond length of Ru curcuminates seems to be longer than the other related structures in the database suggesting its weakeness. A histogram of these Ru−Cl bond distances is depicted in Supporting Information Figure S1, where the red hit belongs to one of the two molecules in the asymmetric unit of the dimethoxycurcumin derivative, shown in Table 1 [Ru−Cl 2.435(1)].[36] The Pt chemotherapy mechanism of action has established Pt−N7(guanine) as necessary for antitumor activity. In addition, a strong deformation of curcumin planarity, similar to that found for curcumin itself in the literature,[49] is apparent in the solid state structure of the title compound, and its interaction with DNA. Using 9-ethylguanine as a model for guanosine, the metal bonding with N7(guanine) in the ruthenium complexes of curcumin and its demethoxylated derivative was validated by ESI-MS studies. These results further demonstrate that the presence or absence of peripheral hydroxy or methoxy groups in curcumin do not greatly influence the interaction of the metal with the β-diketone moiety. This feature is promising for making suitable chemical modifications of the ligand to achieve higher biological activity and lower toxicity. The present study focuses on DNA interaction because previous studies indicate that interaction with DNA bases is highly probable and our results fit such expectation. However, interaction with other targets such as proteins has also been demonstrated[50,51] and should not be excluded for the title compound.

EXPERIMENTAL SECTION

Synthesis and Characterization. Samples for microanalysis were dried in vacuo to constant weight (20 °C, about 0.1 Torr). Elemental analyses (C, H) were performed in house with a Fisons Instruments 1108 CHNS-O elemental analyzer. Electrical conductivity measurements of solutions of the complexes were taken with a Crison CDTM 522 conductimeter at room temperature. IR spectra were recorded from 4000 to 100 cm^{-1} with a Perkin-Elmer System 2000 FTIR instrument. ^{1}H NMR spectra were recorded with a VXR-300 Varian spectrometer. Melting points were determined with an IA 8100 Electrothermal instrument. Positive and negative electrospray mass spectra were obtained with a Series 1100 MSI detector HP spectrometer. Solutions (3 mg/mL) were used for electrospray ionization mass spectrometry (ESI-MS) and data, mass, and intensities were compared to those calculated using IsoPro Isotopic Abundance Simulator, version 2.1.16. Elemental combustion analyses of both compounds confirmed >95% purity.

The commercial natural product curcumin, from Sigma-Aldrich, which is a mixture of curcumin, demethoxycurcumin (d-curcH), and bis(demethoxy)curcumin (bd-curcH), was dissolved (0.368 g, 1 mmol) in methanol (20 mL) and NaOMe (0.054 g, 1 mmol) added. After 1 h stirring at room temperature, $[(p\text{-cymene})RuCl_2]_2$ (0.306 g, 0.5 mmol) was added. The resulting orange solution was stirred at reflux for 24 h. Then solvent was removed in vacuo, the residue redissolved in dichloromethane (10 mL), and the mixture was filtered to remove sodium chloride. The orange solution was concentrated (2 mL) and an orange precipitate afforded, which was

dx.doi.org/10.1021/jm200912j | J. Med. Chem. 2012, 55, 1072−1081

separated, dried under a vacuum, and shown by ESI-MS to be a mixture of (*p*-cymene)ruthenium derivatives, in detail [(*p*-cymene)-Ru(curcuminato)Cl], [(*p*-cymene)Ru(d-curcH)Cl], and [(cymene)-Ru(db-curc)Cl]. ESI-MS (+) CH_3OH (*m*/*z*, relative intensity %): 603 [100] [(*p*-cymene)Ru(curcuminato)]$^+$, 573 [20] [(cymene)Ru(d-curc)]$^+$, 543 [5] [(*p*-cymene)Ru(db-curc)]$^+$. ESI-MS (−) CH_3OH (*m*/*z*, relative intensity %): 367 [100] [curcuminato]$^-$, 337 [20] [d-curc]$^-$, 307 [5] [bd-curc]$^-$. Hence, purification through preparative TLC was carried out by using a mixture of chloroform/methanol in 9:1 ratio as eluent.

[(*p*-Cymene)Ru(curc)Cl] (1), Ru-Cur. The three fractions were separated, and recrystallization in $CHCl_3$ at 4 °C slowly yielded orange−red crystals, which were identified as the pure compound **1**; mp 197−198 °C. Λ_m (CH_3OH, 298 K, 10^{-3} mol/L): 22 S cm^2 mol^{-1}. Λ_m ($(CH_3)_2SO$, 298 K, 10^{-3} mol/L): 2 S cm^2 mol^{-1}. IR (nujol, cm^{-1}): 3220 m br ν(OH), 1619 m, 1591s, 1500vs ν(C═O, C═C). ^{1}H NMR ($CDCl_3$, 293K): δ, 1.39 (d, 6H, CH(CH_3)$_2$ of *p*-cymene), 2.34 (s, 3H, CH_3 of *p*-cymene), 2.98 (m, 1H, CH(CH_3)$_2$ of *p*-cymene), 3.93 (s, 6H, OCH_3 of curc), 5.45 (s, 1H, C(1)*H* of curc), 5.55br, 5.84br (4H, AA′BB′ system, CH_3-C_6H_4-CH(CH_3)$_2$ of *p*-cymene), 6.42 (d, 2H, C(3, 3′)*H* of curc, $^3J_{trans}$ = 15 Hz), 6.91 (br, 2H, C(9, 9′)*H* of curc), 7.00 (br, 4H, C(10, 10′)*H* and C(6, 6′)*H* of curc), 7.52 (d, 2H, C(4, 4′)*H* of curc, $^3J_{trans}$ = 16 Hz). ^{13}C{^{1}H} NMR ($CDCl_3$, 293K): δ, 18.3 (s, CH_3-C_6H_4-CH(CH_3)$_2$), 22.7 (s, CH_3-C_6H_4-CH(CH_3)$_2$), 31.1 (s, CH_3-C_6H_4-CH(CH_3)$_2$), 56.1 (s, O-CH_3 of curc), 79.3, 83.2, 97.8, 99.8 (s, CH_3-C_6H_4-CH(CH_3)$_2$), 102.1 (s, *C*(1, 1′) of curc), 109.3 (s, *C*(6, 6′) of curc), 114.9 (s, *C*(9, 9′) of curc), 122.7 (s, *C*(10, 10′) of curc), 125.6 (s, *C*(5, 5′) of curc), 128.7 (s, *C*(3, 3′) of curc), 138.9 (s, *C*(4, 4′) of curc), 146.9 (s, *C*(7, 7′) of curc), 147.3 (s, *C*(8, 8′) of curc), 178.5 (s, *C*(2, 2′)═O of curc).

[(*p*-Cymene)Ru(d-curc)Cl] (2). Another fraction of the previous separation procedure was identified as the pure compound **2**. It is soluble in alcohols, acetone, acetonitrile, DMSO, and chlorohydrocarbon solvents; mp 196−197 °C. Λ_m (CH_3OH, 298 K, 10^{-3} mol/L): 19 S cm^2 mol^{-1}. Λ_m ($(CH_3)_2SO$, 298K, 10^{-3} mol/L): 3 S cm^2 mol^{-1}. IR (nujol, cm^{-1}): 3225 m br ν(OH), 1619 m, 1590s, 1503vs ν(C═O, C═C). ^{1}H NMR (CD_3OD, 293K): δ, 1.40 (d, 6H, CH(CH_3)$_2$ of *p*-cymene, ^4J = 7 Hz), 2.32 (s, 3H, CH_3 of *p*-cymene), 2.92 (m, 1H, CH(CH_3)$_2$ of *p*-cymene), 3.90 (s, 3H, OCH_3 of d-curc), 5.59d, 5.75d (4H, AA′BB′ system, CH_3-C_6H_4-CH(CH_3)$_2$ of *p*-cymene, ^3J = 6 Hz), 5.65 (s, 1H, C(1)*H* of d-curc), 6.64 (d, 2H, C(3, 3′)*H* of d-curc, $^3J_{trans}$ = 18 Hz), 6.89 (d, 2H, C(9, 9′)*H* of d-curc, ^3J = 8 Hz), 7.15 (d, 1H, C(6)*H* of d-curc, ^3J = 8 Hz), 7.23 (s, 1H, C(6′)*H* of d-curc), 7.23 (s, 1H, C(6′)*H* of d-curc), 7.53 (d, 2H, C(4, 4′)*H* of d-curc, $^3J_{trans}$ = 8 Hz), 7.61 (d, 1H, C(7)*H* of d-curc, ^3J = 8 Hz), 7.67 (d, 4H, C(10, 10′)*H* of d-curc, ^3J = 8 Hz). ^{13}C{^{1}H} NMR (CD_3OD, 293K): δ, 18.6 (s, CH_3-C_6H_4-CH(CH_3)$_2$), 22.5 (s, CH_3-C_6H_4-CH(CH_3)$_2$), 31.9 (s, CH_3-C_6H_4-CH(CH_3)$_2$), 56.5 (s, O-CH_3 of d-curc), 79.7, 82.2, 99.0, 100.7 (s, CH_3-C_6H_4-CH(CH_3)$_2$), 102.6 (s, *C*(1, 1′) of d-curc), 107.4 (s, *C*(6, 6′) of d-curc), 116.7 (s, *C*(9, 9′) of d-curc), 124.2 (s, *C*(10, 10′) of d-curc), 125.3 (s, *C*(5, 5′) of d-curc), 130.5 (s, *C*(3, 3′) of d-curc), 137.2 (s, *C*(4, 4′) of d-curc), 145.3 (s, *C*(7, 7′) of d-curc), 147.0 (s, *C*(8, 8′) of d-curc), 177.8 (s, *C*(2, 2′)═O of d-curc).

Diffraction Study. Suitable crystals for X-ray diffraction data were obtained by dissolving the samples in a mixture of 1:1 dichloromethane/ethanol solutions and on standing at room T for a week. Data were collected at 125K using a Bruker SMART APEX II CCD X-ray diffractometer. Structure resolution and refinement were performed with SHELXTL,[52] details are included in Table 3. H atoms were calculated and constrained as riding on their bound atoms. CCDC833577 contains the supplementary crystallographic data for this paper. These data can be obtained free of charge from The Cambridge Crystallographic Data Centre via www.ccdc.cam.ac.uk/data_request/cif.

Theoretical Study. The theoretical study involved calculations using software programs from Accelrys.[53] Density functional theory code DMol3 was applied to calculate energy, geometry, and frequencies implemented in Materials Studio 5.5 (PC platform).[54] We employed the double numerical polarized (DNP) basis set that includes all the occupied atomic orbitals plus a second set of valence atomic orbitals, and polarized d-valence orbitals,[55] and correlation generalized gradient approximation (GGA) was applied in the manner suggested by Perdew−Burke−Ernzerhof (PBE),[56] these are the conditions for the highest-accuracy level in DMol3. The spin unrestricted approach was exploited with all electrons considered explicitly. The real space cutoff of 5 Å was imposed for numerical integration of the Hamiltonian matrix elements. The self-consistent-field convergence criterion was set to the root-mean-square change in the electronic density to be less than 10^{-6} electron/Å^3. The convergence criteria applied during geometry optimization were 2.72 × 10^{-4} eV for energy and 0.054 eV/ Å for force.

Table 3. Crystal Data and Structure Refinement for (*p*-Cymene)Ru(curcuminato)chloro·0.5H_2O

empirical formula	$C_{31}H_{32}ClO_6Ru$, 0.5H_2O
formula weight	1292.19
temperature	125(2)K
wavelength	0.71073 Å
crystal system	orthorhombic
space group	*Pbcn*
unit cell dimensions	*a* = 23.036(7) Å
	b = 11.367(4) Å
	c = 22.354(7) Å
volume	5853(3) Å^3
Z	8
density (calcd)	1.466 mg/m^3
absorption coefficient	0.671 mm^{-1}
F(000)	2656
crystal size	0.34 × 0.26 × 0.06 mm^3
θ range for data collection	2.00−19.61°
index ranges	$-21 \le h \le 21$, $-10 \le k \le 10$, $-21 \le l \le 21$
reflns collected	32685
independent reflections	2580 [*R*(int) = 0.1308]
completeness to θ = 19.61°	99.8%
absorption correction	empirical
max and min transmission	0.9609 and 0.8041
refinement method	full-matrix least-squares on F^2
data/restraints/parameters	2580/82/208
goodness-of-fit on F^2	1.082
final *R* indices [$I > 2\sigma(I)$]	*R*1 = 0.0838, *wR*2 = 0.1921
R indices (all data)	*R*1 = 0.1268, *wR*2 = 0.2184
largest diff. peak and hole	1.023 and −0.562 e·Å^{-3}

Cell Lines and in Vitro Culture Conditions. The cell lines MCF7 (HTB-22, human breast adenocarcinoma), HCT116 (CCL-247, human colorectal carcinoma), A549 (CCL-185, human lung carcinoma), and U-87 MG (HTB-1, human glioblastoma) were obtained from ATCC (American Type Culture Collection, Manassas, VA, USA); A2780 human ovarian carcinoma were obtained from ECACC (European Collection of Animal Cell Culture, Salisbury, U.K.). They were maintained under standard culture conditions (37 °C; 5% CO_2) in DMEM medium (Euroclone, Milan, Italy), supplemented with 10% fetal calf serum (Euroclone, Milan, Italy), 1% glutamine, and 1% antibiotics mixture; for HCT116 and U-87 MG cells, 1% sodium pyruvate and 1% nonessential amino acids (both from Sigma-Aldrich, Milan, Italy) were also added to the culture medium. CP8 cells (so-called because of their ability to grow in medium containing 8 μM cisplatin), developed by chronic exposure of the parental A2780 cisplatin-sensitive line to increasing concentrations of cisplatin, were obtained from Dr. R. Ozols (Fox Chase Cancer Center, Philadelphia, PA).[57] MCF-10A (a cell line derived from human mammary epithelium, spontaneously immortalized) was

obtained from ATCC and maintained in a 1:1 mixture of Ham's F12 and DMEM (Euroclone, Milan, Italy), supplemented with 5% horse serum and 1% penicillin/streptomycin (Euroclone, Milan, Italy) and with 0.5 mg/mL hydrocortisone, 10 μg/mL insulin,, and 20 ng/mL recombinant human EGF (all three from Sigma-Aldrich, Milan, Italy). All experiments were performed within 10 passages from thawing.

Drugs. The title compound was reconstituted in sterile DMSO at a concentration of 1 M; stock solutions were then diluted to the desired final concentrations with sterile complete medium immediately before each experiment. The final DMSO concentration never exceeded 0.2%, which was not toxic to the cells under the drug exposure conditions used in this study.

Growth Inhibition Assay. The 3-(4,5-dimethylthiazol-2-yl)-2,5-diphenyltetrazolium bromide (MTT) assay was performed on all the cell lines tested as described[58] with minor modifications. Briefly, according to the growth profiles previously defined for each cell line, adequate numbers of cells were plated in each well of a 96-well plate in 0.1 mL of complete culture medium and allowed to attach for 24 h. Cells were exposed at 37 °C for 72 h to the title compound at concentrations ranging between 5 and 750 nm, bringing the final volume in each well to 0.2 mL. Each experiment included 8 replications per concentration tested; control samples were run with 0.2% DMSO. At the end of the period of incubation with the title compound, MTT (0.05 mL of a 2 mg/mL stock solution in PBS) was added to each well for 3 h at 37 °C. Cell supernatants were then carefully removed, the blue formazan crystals formed through MTT reduction by metabolically active cells were dissolved in 0.1 mL of DMSO, and the corresponding optical densities were measured at 570 nm, using a universal microplate reader EL800 (Bio-TekWinooski, VT). IC_{50} values were estimated from the resulting concentration−response curves by nonlinear regression analysis, using GraphPad Prism software, version 4.03. (GraphPad, San Diego, CA, USA). Differences between IC_{50} values were analyzed statistically by analysis of variance with Bonferroni post-test for multiple comparisons.

Docking on DNA. Docking studies were performed with the molecular mechanics CDOCKER package in Discovery Studio 3.0 from Accelrys.[53] CDOCKER is a grid-based molecular docking method that employs CHARMm.[59] Curcumin was geometry optimized using the density functional theory (DFT) code DMol3 included in Materials Studio version 5.5 from Accelrys, using the same setting earlier described for the (*p*-cymene)Ru(curcuminato)chloro complex. Initial docking of curcumin was performed on a DNA species deposited in the Protein Data Bank www.pdb.org (code 1AU7).[49] CDOCKER was used to dock curcumin into the double helix. The simulation was performed using a binding site sphere of radius 12 Å centered in the minor groove of the receptor. An excellent agreement was obtained compared to published results as the best docked pose showed important binding features mostly based on interactions due to both peripheral moieties of curcumin including its twisted structural features.[49] Solvation of this receptor, including counterions, was performed and 1610 molecules of water, 22 Na^+ and 4 Cl^- were obtained. Therefore, the 18 negative DNA phosphate charges were balanced with 18 positive charges, making the receptor neutral. The center of a 12 Å radius sphere, defined as the midpoint between O(phosphate- cytosine3-"S") and O(phosphate- cytosine3-"A"), was located in the major groove. The main purpose of the solvation protocol was to include counterions, and so these added waters were later removed. An initial docking of curcumin was performed requesting 10 poses. In 9 out of 10 poses, the keto−enol curcumin moiety was not positioned toward the DNA, rather the DNA−curcumin interaction was based on peripheral O(curcumin) atoms and curcumin loss of planarity, as indicated above for 1AU7.[49] This feature provides support for our next docking procedure for a Ru−curcumin complex, e.g.. for the metal coordinated to the keto−enol moiety and not, initially, involved in DNA binding while preserving peripheral interactions of curcumin with DNA. Additional docking for 100 poses was performed, confirming such statistics. Pose 21, suggested a potential H(enol)−N7(guanine-"A") approach and was selected. The complex (*p*-cymene)Ru(curcuminato)chloro, previously geometry optimized with DMol3, was curcuminato superimposed onto the originally docked curcumin, while holding its Ru(*p*-arene)Cl environment, and the free curcumin was eliminated. Because the CHARMm force field does not contain bonding parameters for Ru, the metal was treated as an ion (Ru^{2+}). To account for the Ru coordination sphere, we set (1) a flat-bottomed distance restraint between Ru and the center of *p*-cymene ring using a force constant of 200 kcal/(mol·Å^2) and an upper threshold of 1.90 Å, so that a closely related Ru-arene distance could be kept while allowing *p*-cymene rotation during docking; (2) a rigid-body harmonic restraint to Ru−curcuminato chelate moiety using a force constant of 10 kcal/(mol·Å^2), conserved planarity of the 6-membered Ru−curcuminato ring, with one O atom having a negative charge (anion) and the other set as a neutral carbonyl; (3) the Cl as an anion. Throughout this process, we wanted to be sure that the approach of the Ru complex to the DNA decamer receptor was not chemically affected before entering the groove. Subsequently, we eliminated DNA counterions and performed a new solvation-counterion generation, eliminated all water molecules and performed a minimization of this counterion-decamer-Ru-complex-pose-21 system, having the receptor and counterions fixed.

Conditions for minimizations were as follows: The Smart Minimizer algorithm performed 1000 steps of Steepest Descent with a rms gradient tolerance of 3, followed by 1000 steps of Conjugate Gradient minimization with a rms gradient tolerance of 0.1. This simulation used a Distance-Dependent Dielectric Constant of 4, and all other parameters were default conditions.

This showed Ru−Cl of 2.72 Å, Ru−O(anionic) 2.158 Å, Ru−O(carbonyl) 2.250 Å, and Ru−centroid 2.028 Å; potential energy was −7.9 kcal/mol, electrostatic energy, −85.6 kcal/mol, and vdW energy 11.0 kcal/mol. The same constraints were applied to the standard dynamic cascade protocol shown in Supporting Information Figure S2. Conditions were set as follows: a first minimization used the Steepest Descent algorithm with 500 steps and rms gradient tolerance of 0.1. A second minimization used a Conjugate Gradient algorithm of 500 steps and rms gradient of 0.0001. The heating process used 100000 steps of time step 0.001, initial temperature was 50K, and target temperature was 300K. The equilibration process used 10000 steps with time step 0.001 and target temperature of 300K. The production process was of 500000 steps, equivalent to 0.5 ns, with time step 0.001 and target temperature of 300K; the production stage was carried out under an NVT setting, which is a constant temperature dynamics using Berendsen weak coupling method. The simulation used a distance-dependent dielectrics with a dielectric constant of 4; all other parameters were default conditions. Supporting Information Figure S3 shows conformation no. 60, which has the lowest energy. A similar standard dynamic cascade was performed for the receptor having more flexibility: (1) DNA with all bases free, excepted both terminal pairs, and all phosphate and ribose fixed; (2) Ru(II) cation; (3) Ru−centroid distance restraint with force constant (100 kcal/(mol·Å^2)) and threshold (1.90 Å); (4) Ru−curcuminato chelate, harmonic restraint, best-fit, force constant (10 kcal/(mol·Å^2)), with one O atom negatively charged (anion) and the other as a carbonyl; (5) Cl as an anion taken out of the coordination sphere (Ru---Cl = 8.9 Å). Supporting Information Figure S4 shows the pattern of potential energy vs conformations. We selected conformer no. 155 as a good candidate for further study, Supporting Information Figure S5. Its minimized structure (Figure 6) shows a good approach of Ru to N7(guanine)(2.824 Å). Comparing Supporting Information Figure S5 with Supporting Information Figure S3 one can see that one H-bond between bases is lost, in the former, due to the greater flexibility imposed.

Because some conformers show also some potential approach for O(phosphate) of guanine6 ("A") we also investigated this feature. A longer simulation (1 ns) was performed, and the resulting 500 conformations are shown in Supporting Information Figure S6. We focused on conformer no. 351 (Supporting Information Figure S7), selected it, and performed a minimization (Figure 7). The energy of both potential candidates of interaction for the Ru-complex with this DNA decamer, Ru−N7 bond (Figure 6) and Ru−O(phosphate) (Figure 7), were obtained using the same condition of minimizations,

they are 263.8 and 263.4 kcal/mol, respectively. Such a small difference cannot discriminate between these conformers.

■ ASSOCIATED CONTENT

Supporting Information

Histogram of the Ru−Cl bond length from the CSD data. Docking plot of potential energy vs time for the production stage for the Ru-complex on a B DNA C-G decamer. Conformation no. 60 from Docking. Potential energy vs conformations, showing conformation no. 155. Selected atoms for conformation no. 155 from previous cascade. Standard dynamic cascade search for potential Ru−O(phosphate) interaction. Conformer no. 351, showing potential Ru−O(phosphate) interaction. Dose-dependence of the title compound on 5 tumor cell lines. This material is available free of charge via the Internet at http://pubs.acs.org.

■ AUTHOR INFORMATION

Corresponding Author

*(F.C.) Phone: 39 06 49913632. E-mail: caruso@vassar.edu. (M.R.) Phone: 1 845 4377134. E-mail: rossi@vassar.edu.

■ ACKNOWLEDGMENTS

Financial support by Università degli Studi di Camerino, Consiglio Nazionale delle Ricerche CNR—Rome, Research Committee and URSI program at Vassar College. M.R. thanks the U.S. National Science Foundation, through grant 0521237 for the X-ray diffractometer, and Howard Hughes Medical Institute for grant 52006322.

■ ABBREVIATIONS USED

DFT, density functional theory; ESI-MS, electron spray resonance mass spectrometry; Ru-Cur, (**1**), (*p*-cymene)Ru(curcuminato)chloro; Ru-dim-Cur, (*p*-cymene)Ru(dimethoxycurcuminato)chloro; curcH, curcumine; d-curcH, demethoxycurcumin; bd-curcH, bis-demethoxycurcumin

■ REFERENCES

(1) *Global Cancer—Facts & Figures*; American Cancer Society: Atlanta, GA, 2007; 1.
(2) Guo, Z.; Sadler, P. J. Metals in medicine. *Angew. Chem., Int. Ed.* **1999**, *38*, 1512−1531.
(3) Galanski, M.; Jakupec, M. A.; Keppler, B. K. Update of the preclinical situation of anticancer platinum complexes: novel design strategies and innovative analytical approaches. *Curr. Med. Chem.* **2005**, *12*, 2075−2094.
(4) Reedijk, J. Platinum anticancer coordination compounds: study of DNA binding inspires new drug design. *Eur. J. Inorg. Chem.* **2009**, 1303−1302.
(5) Ronconi, L.; Sadler, P. J. Using coordination chemistry to design new medicines. *Coord. Chem. Rev.* **2007**, *251*, 1633−1648.
(6) Bratsos, I.; Jedner, S.; Gianferrara, T.; Alessio, E. Ruthenium anticancer compounds: challenges and expectations. *Chimia* **2007**, *61*, 692−697.
(7) Hartinger, C. G.; Jakupec, M. A.; Zorbas-Seifried, S.; Kynast, B.; Zorbas, H.; Keppler, B. K. A from bench to bedside—preclinical and early clinical of the anticancer agent imidazolium *trans*-tetrachlorobis(1*H*-indazole)ruthenate(III). *Chem. Biodivers.* **2008**, *5*, 2140−2155.
(8) Yan, Y. K.; Melchart, M.; Habtemariam, A.; Sadler, P. J. Organometallic chemistry, biology and medicine: ruthenium arene anticancer complexes. *Chem. Commun.* **2005**, 4764−4776.
(9) Reedijk, J. Metal−ligand exchange kinetics in platinum and ruthenium complexes. Significance for effectiveness as anticancer drugs. *Platinum Met. Rev.* **2008**, *52*, 2−11.
(10) Dyson, P. J.; Sava, G. Metal-based antitumor drugs in the post genomic era. *J. Chem. Soc., Dalton Trans.* **2006**, 1929−1933.
(11) Dougan, S. J.; Sadler, P. J. The design of organometallic rutheniumarene anticancer agents. *Chimia* **2007**, *61*, 704−715.
(12) Dyson, P. J. Systematic design of a targeted organometallic antitumor drug in pre-clinical development. *Chimia* **2007**, *61*, 698−703.
(13) Suss-Fink, G. Arene ruthenium complexes as anticancer agents. *J. Chem. Soc., Dalton Trans.* **2010**, *39*, 1673−1688.
(14) Pizarro, A. M.; Habtemariam, A.; Sadler, P. J. Activation mechanisms for organometallic anticancer agents. *Top. Organomet. Chem.* **2010**, *32*, 21−56.
(15) Morris, R. E.; Aird, R. E.; Murdoch, P. D. S; Chen, H.; Cummings, J.; Hughes, N. D.; Parsons, S.; Parkin, A.; Boyd, G.; Jodrell, D. I.; Sadler, P. J. Inhibition of cancer cell growth by ruthenium(II) arene complexes. *J. Med. Chem.* **2001**, *44*, 3616−3621.
(16) Aird, R. E.; Cummings, J.; Ritchie, A. A.; Muir, M.; Morris, R. E.; Chen, H.; Sadler, P. J.; Jodrell, D. I. In vitro and in vivo activity and cross resistance profiles of novel ruthenium (II) organometallic arene complexes in human ovarian cancer. *Br. J. Cancer* **2002**, *86*, 1652−1657.
(17) Novakova, O.; Chen, H.; Vrana, O.; Rodger, A.; Sadler, P. J.; Brabec, V. Competition between glutathione and guanine for a ruthenium(II) arene anticancer complex: detection of a sulfenatointermediate. *Biochemistry* **2003**, *42*, 11544−11554.
(18) Chen, H.; Parkinson, J. A.; Morris, R. E.; Sadler, P. J. Highly selective binding of organometallic ruthenium ethylenediamine complexes to nucleic acids: novel recognition mechanisms. *J. Am. Chem. Soc.* **2003**, *125*, 173−186.
(19) Wang, F.; Chen, H.; Parkinson, J. A.; Murdoch, P. D. S.; Sadler, P. J. Reactions of a ruthenium(II) arene antitumor complex with cysteine and methionine. *Inorg. Chem.* **2002**, *41*, 4509−4523.
(20) Wang, F.; Bella, J.; Parkinson, J. A.; Sadler, P. J. Competitive reactions of a ruthenium arene anticancer complex with histidine, cytochrome c and an oligonucleotide. *J. Biol. Inorg. Chem.* **2005**, *10*, 147−155.
(21) Wang, F.; Xu, J.; Habtemariam, A.; Bella, J.; Sadler, P. J. Competition between glutathione and guanine for a ruthenium(II) arene anticancer complex: detection of a sulfenatointermediate. *J. Am. Chem. Soc.* **2005**, *127*, 17734−17743.
(22) Fernandez, R.; Melchart, M.; Habtemariam, A.; Parsons, S.; Sadler, P. J. Use of chelating ligands to tune the reactive site of half-sandwich ruthenium(II)−arene anticancer complexes. *Chem.—Eur. J.* **2004**, *10*, 5173−5179.
(23) Habtemariam, A.; Melchart, M.; Fernandez, R.; Parsons, S.; Oswald, I. D. H.; Parkin, A.; Fabbiani, F. P. A; Davidson, J. E.; Dawson, A.; Aird, R. E.; Jodrell, D. I.; Sadler, P. J. Structure−activity relationships for cytotoxic ruthenium(II) arene complexes containing *N,N*-, *N,O*-, and *O,O*-chelating ligands. *J. Med. Chem.* **2006**, *49*, 6858−6868.
(24) Ang, W. H.; Daldini, E.; Scolaro, C.; Scopelliti, R.; Juillerat-Jeanneret, L.; Dyson, P. J. Development of organometallic ruthenium−arene anticancer drugs that resist hydrolysis. *Inorg. Chem.* **2006**, *45*, 9006−9013.
(25) Vock, C. A.; Renfrew, A. K.; Scopelliti, R.; Juillerat-Jeanneret, L.; Dyson, P. J. Influence of the diketonato ligand on the cytotoxicities of [Ru(eta-$_6$-*p*-cymene)(R_2acac)(PTA)]+ complexes (PTA = 1,3,5-triaza-7-phosphaadamantane). *Eur. J. Inorg. Chem.* **2008**, 1661−1667.
(26) Valentini, A.; Conforti, F.; Crispini, A.; De Martino, A.; Condello, R.; Stellitano, C.; Rotilio, G.; Ghedini, M.; Federici, G.; Bernardini, S.; Pucci, D. Synthesis, oxidant properties, and antitumoral effects of a heteroleptic palladium(II) complex of curcumin on human prostate cancer cells. *J. Med. Chem.* **2009**, *52*, 484−491.
(27) Pucci, D.; Bloise, R.; Bellusci, A.; Bernardini, S.; Ghedini, M.; Pirillo, S.; Valentini, A.; Crispini, A. Curcumin and cyclopalladated complexes: a recipe for bifunctional biomaterials. *J. Inorg. Biochem.* **2007**, *101*, 1013−1022.

(28) Ferrari, E.; Lazzari, S.; Marverti, G.; Pignedoli, F.; Spagnolo, F.; Saladini, M. Synthesis, cytotoxic, and combined cDDP activity of new stable curcumin derivatives. *Bioorg. Med. Chem.* **2009**, *17*, 3043−3052.
(29) Song, X. Y.-M.; Xu, J.-P.; Ding, L.; Hou, Q.; Liu, J.-W.; Zhu, Z.-L. Syntheses, characterization and biological activities of rare earth metal complexes with curcumin and 1,10-phenanthroline-5,6-dione. *J. Inorg. Biochem.* **2009**, *103*, 396−400.
(30) Anand, P.; Thomas, S. G.; Kunnumakkara, A. B.; Sundaram, C.; Harikumar, K. B.; Sung, B.; Tharakan, S. T.; Misra, K.; Priyadarsini, I. K.; Rajasekharan, K. N.; Aggarwal, B. B. Biological activities of curcumin and its analogues (Congeners) made by man and Mother Nature. *Biochem. Pharmacol.* **2008**, *76*, 1590−1611.
(31) Aggarwal, B. B.; Sundaram, C.; Malani, N.; Ichikawa, H. Curcumin: the Indian solid gold. *Adv. Exp. Med. Biol.* **2007**, *595*, 1−75.
(32) Yang, F.; Lim, P. L. G. P.; Begum, A. N.; Ubeda, O. J.; Simmons, M. R.; Ambegaokar, S. S.; Chen, P.; Kayed, R.; Glabe, C. G.; Frautschy, S. A.; Cole, G. M. Curcumin inhibits formation of amyloid beta oligomers and fibrils, binds plaques, and reduces amyloid in vivo. *J. Biol. Chem.* **2005**, *280*, 5892−5901.
(33) Garcia-Alloza, M.; Borrelli, L. A.; Rozkalne, A.; Hyman, B. T.; Bacskai, B. J. Curcumin labels amyloid pathology in vivo, disrupts existing plaques, and partially restores distorted neurites in an Alzheimer mouse model. *J. Neurochem.* **2007**, *102*, 1095−1104.
(34) Marchetti, F.; Pettinari, C.; Pettinari, R.; Cerquetella, A.; Cingolani, A.; Chan, E. J.; Kozawa, K.; Skelton, B. W.; White, A. H.; Wanke, R.; Kuznetsov, M. L.; Martins, L. M. D. R. S.; Pombeiro, A. J. L. Areneruthenium(II) 4-acyl-5-pyrazolonate derivatives: coordination chemistry, redox properties, and reactivity. *Inorg. Chem.* **2007**, *46*, 8245−8257.
(35) Fernández, R.; Melchart, M.; Habtemariam, A.; Parsons, S.; Sadler, P. J. Use of chelating ligands to tune the reactive site of half-sandwich ruthenium(II)−arene anticancer complexes. *Chem.—Eur. J.* **2004**, *10*, 5173−5179.
(36) Kuhlwein, F.; Polborn, K.; Beck, W. Metal complexes of dyes. Part 9. Transition metal complexes of curcumin and derivatives. *Z. Anorg. Allg. Chem.* **1997**, *623*, 1211−1219.
(37) Wang, F.; Habtemariam, A.; van der Geer, E. P. L; Deeth, R. J.; Gould, R. T.; Parsons, S.; Sadler, P. J. Synthesis, characterization, and reaction pathways for the formation of a GMP adduct of a cytotoxic thiocyanatorutheniumarene complex. *J. Biol. Inorg. Chem.* **2009**, *14*, 1065−1076.
(38) Vock, C. A.; Renfrew, A. K.; Scopelliti, R.; Juillerat-Jeanneret, L.; Dyson, P. J. Influence of the diketonato ligand on the cytotoxicities of $[Ru(\eta^6\text{-}p\text{-cymene})(R_2acac)(PTA)]^+$ complexes (PTA = 1,3,5-triaza-7-phosphaadamantane). *Eur. J. Inorg. Chem.* **2008**, 1661−1671.
(39) Hayward, R. L.; Schornagel, Q. C.; Tente, R.; Macpherson, J. S.; Aird, R. E.; Guichard, S.; Habtemariam, A.; Sadler, P. J.; Jodrell, D. I. Investigation of the role of Bax, p21/Waf1 and p53 as determinants of cellular responses in HCT116 colorectal cancer cells exposed to the novel cytotoxic ruthenium(II) organometallic agent, RM175. *Cancer Chemother. Pharmacol.* **2005**, *55*, 577−583.
(40) Schuecker, R.; John, R. O.; Jakupec, M. A.; Arion, V. B.; Keppler, B. K. Water-soluble mixed-ligand ruthenium(II) and osmium(II) arene complexes with high antiproliferative activity. *Organometallics* **2008**, *27*, 6587−6595.
(41) Filak, L. K.; Muehlgassner, G.; Bacher, F.; Roller, A.; Galanski, M.; Jakupec, M. A.; Keppler, B. K.; Arion, V. B. Ruthenium− and osmium−arene complexes of 2-substituted indolo[3,2-*c*]quinolines: synthesis, structure, spectroscopic properties, and antiproliferative activity. *Organometallics* **2011**, *30*, 273−283.
(42) Boyer, J. C.; Umar, A.; Risinger, J. I.; Lipford, J. R.; Kane, M.; Yin, S.; Barrett, J. C.; Kolodner, R. D.; Kunkel, T. A. Microsatellite instability, mismatch repair deficiency, and genetic defects in human cancer cell lines. *Cancer Res.* **1995**, *55*, 6063−6070.
(43) Fink, D.; Nebel, S.; Aebi, S.; Zheng, H.; Cenni, B.; Nehmé, A.; Christen, R. D.; Howell, S. B. The role of DNA mismatch repair in platinum drug resistance. *Cancer Res.* **1996**, *56*, 4881−4886.
(44) Behrens, B. C.; Hamilton, T. C.; Masuda, H.; Grotzinger, K. R.; Whang-Peng, J.; Louie, K. G.; Knutsen, T.; McKoy, W. M.; Young, R. C.; Ozols, R. F. Characterization of a *cis*-diamminedichloroplatinum-(II)-resistant human ovarian cancer cell line and its use in evaluation of platinum analogues. *Cancer Res.* **1987**, *47*, 414−418.
(45) Colella, G.; Pennati, M.; Bearzatto, A.; Leone., R.; Colangelo., D.; Manzotti, C.; Daidone., M. G.; Zaffaroni, N. Activity of a trinuclear platinum complex in human ovarian cancer cell lines sensitive and resistant to cisplatin: cytotoxicity and induction and gene-specific repair of DNA lesions. *Br. J. Cancer.* **2001**, *84*, 1387−1390.
(46) Chen, H.; Wang, F.; Parkinsons, J. A.; Parsons, R. A.; Coxal, R. A.; Gould, R. O.; Sadler, P. J. Organometallic ruthenium(II) diamine anticancer complexes: arene-nucleobase stacking and stereospecific hydrogen-bonding in guanine adducts. *J. Am. Chem. Soc.* **2002**, *124*, 3064−3082.
(47) Liu, H.-K.; Wang, F.; Parkinsons, J. A.; Bella, J.; Sadler, P. J. Ruthenation of duplex and single-stranded d(CGGCCG) by organometallic anticancer complexes. *Chem.—Eur. J.* **2006**, *12*, 6151−6165.
(48) Melchart, M.; Habtemariam, A.; Parsons, S.; Sadler, P. J. Chlorido-, aqua-, 9-ethylguanine- and 9-ethyladenine-adducts of cytotoxic ruthenium arene complexes containing *O*,*O*-chelating ligands. *J. Inorg. Biochem.* **2007**, *101*, 1903−1912.
(49) Zsila, F.; Zsolt, B.; Miklós, S. M. Circular dichroism spectroscopic studies reveal pH dependent binding of curcumin in the minor groove of natural and synthetic nucleic acids. *Org. Biomol. Chem.* **2004**, *2*, 2902−2910.
(50) Messori, L.; Vilchez, F.; Gonzales.; Vilaplana, R.; Piccioli, F.; Alessio, E.; Keppler, B. Binding of antitumor ruthenium(III) complexes to plasma proteins. *Metal-Based Drugs* **2000**, *7*, 335−342.
(51) Martínez, A.; Suárez, J.; Shand, T.; Magliozzo, R. S.; Sánchez-Delgado, R. A. Interactions of arene−Ru(II)−chloroquine complexes of known antimalarial and antitumor activity with human serum albumin (HSA) and transferrin. *J. Inorg. Biochem.* **2011**, *105*, 39−45.
(52) Sheldrick, G. M. *SHELXTL, An Integrated System for Solving, Refining and Displaying Crystal Structures from Diffraction Data*; University of Gottingen: Gottingen, Germany, 1981.
(53) *Discovery Studio 3.0*; Accelrys, Inc.: 10188 Telesis Court, Suite 100, San Diego, CA 92121, USA.
(54) Delley, B. From molecules to solids with the DMol3 approach. *J. Chem. Phys.* **2000**, *113*, 7756−7764.
(55) Perdew, J. P.; Chevary, J. A.; Vosko, S. H.; Jackson, K. A.; Pederson, M. R.; Singh, D. J.; Fiolhais, C. Atoms, molecules, solids, and surfaces: applications of the generalized gradient approximation for exchange and correlation. *Phys. Rev. B: Condens. Matter Mater. Phys.* **1992**, *46*, 6671−6687.
(56) Becke, A. D. Density-functional exchange-energy approximation with correct asymptotic behavior. *Phys Rev. A.* **1988**, *38*, 3098−3100.
(57) Behrens, B. C.; Hamilton, T. C.; Masuda, H.; Grotzinger, K. R.; Whang-Peng, J.; Louie, K. G.; Knutsen, T.; McKoy, W. M.; Young, R. C.; Ozols, R. F. Characterization of a *cis*-diamminedichloroplatinum-(II)-resistant human ovarian cancer cell line and its use in evaluation of platinum analogues. *Cancer Res.* **1987**, *47*, 414−418.
(58) Scudiero, D. A.; Shoemaker, R. H.; Paull, K. D.; Monks, A.; Tierney, S.; Nofziger, T. H.; Currens, M. J.; Seniff, D.; Boyd, M. R. Evaluation of a soluble tetrazolium/formazan assay for cell growth and drug sensitivity in culture using human and other tumor cell lines. *Cancer Res.* **1988**, *48*, 4827−4833.
(59) Wu, G.; Robertson, D. H.; Brooks, C. L. III; Vieth, M. Detailed analysis of grid-based molecular docking: a case study of CDOCKER−CHARMm based MD docking algorithm. *J. Comput. Chem.* **2003**, *24*, 1549−1562.